Mode transition for power dissipation induced by driving frequency in capacitively coupled plasma

S. J. You, H. C. Kim,[a] C. W. Chung,[b] H. Y. Chang, and J. K. Lee[a]
Department of Physics, Korea Advanced Institute of Science and Technology, Daejeon 305-701, South Korea

(Received 29 May 2003; accepted 2 September 2003)

We measured electrical characteristics of capacitively coupled plasma at low pressure (2.67 Pa) with different driving frequencies. From these measurements, we observed a significant change in discharge power characteristics during the frequency increase. While increasing the frequency, a square dependence of power characteristics ($P \sim I^2$) changes to a linear dependence ($P \sim I$). This observed result reflects that a power dissipation mode transition from an ion-dominated dissipation mode to an electron-dominated dissipation mode takes place during the driving frequency increase. Both the results calculated from a simple sheath model and a particle-in-cell simulation are in a good agreement with the experimental data. © *2003 American Institute of Physics.*
[DOI: 10.1063/1.1621085]

I. INTRODUCTION

Radio-frequency (rf) capacitive discharge is widely used in semiconductor processing and numerous studies have been conducted in various related areas.[1–9] There are many mode transitions in a capacitive discharge, such as collisionless to collisional heating mode transition,[5,6] α to γ mode transition,[7] and electron to ion power dissipation mode transition.[8–10] Among these, the electron to ion power dissipation mode transition has been investigated by Beneking,[8] Godyak *et al.*,[9,11] and You *et al.*[10] There are two ways to consume the rf discharge power in a capacitive discharge. One is a power dissipation conducted by electrons in a bulk plasma, the other is a power dissipation conducted by ions in a sheath. When a discharge current is small, electrons in the bulk plasma mainly consume the discharge power so that the discharge power is almost proportional to the current ($P_{\mathrm{dis}} \sim P_{\mathrm{bulk}} = V_p \cdot I$). However, when a discharge current is large, ions in the sheath mainly consume the discharge power so that the discharge power is almost proportional to I^2 ($P_{\mathrm{dis}} \sim P_{\mathrm{sheath}} = R_{\mathrm{sh}} \cdot I^2$).[8,9,11] Therefore, as the discharge current increases, an evolution of the current/power characteristic, $P(I)$, from a linear to a square dependence on the current is observed. This evolution represents the transition of the power dissipation mode from electron-dominated dissipation mode to the ion-dominated dissipation mode.[9,11] There have been many experimental investigations into the transition of the power dissipation mode induced by current, gas pressure,[9,11] and magnetic field.[10] But, there have not been any experimental studies of the frequency dependent effect on the transition. It has just been briefly suggested in Refs. 8 and 11 without any experimental verification.

In this study, we experimentally investigate the driving frequency effect on the transition. We present an evolution of the power characteristic from a square one ($P \sim I^2$) to a linear one ($P \sim I$) as the frequency increases. It reflects a transition of the power dissipation mode from an ion-dominated dissipation mode to an electron-dominated dissipation mode during a frequency increase. A driving frequency dependency of the capacitive rf sheath resistance gives a clue to understanding the transition. Using a simple power dissipation model including the collisional sheath,[8–10] we can calculate the power characteristics of the discharge and theoretically evaluate the mode transition against the driving frequency. Furthermore, through the particle-in-cell (PIC) simulation, we obtain dissipated rf power for each species at various frequencies, so that we can theoretically confirm the transition.

II. EXPERIMENTAL DETAILS

The experiment is performed in a capacitive discharge reactor, as shown in Fig. 1. The reactor is asymmetrically driven at different frequencies (8 MHz to 30 MHz), with argon, and two different size electrodes. The lower one is the grounded electrode (200 mm) and the upper one is the powered electrode (140 mm). The two electrodes are separated

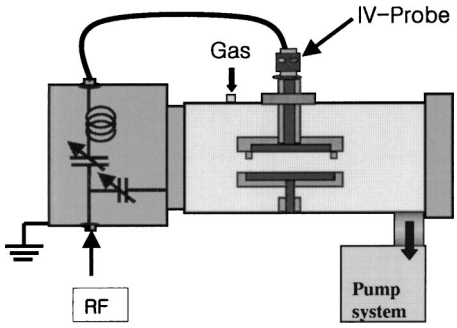

FIG. 1. Experimental setup of the capacitively coupled plasma.

[a]Also at: Department of Electronic and Electrical Engineering, Pohang University of Science and Technology, Pohang 790-784, South Korea.
[b]Corresponding author; also at: Division of Electrical and Computer Engineering, Hanyang University, Seoul, 133-791, South Korea, electronic mail: joykang@hananet.edu

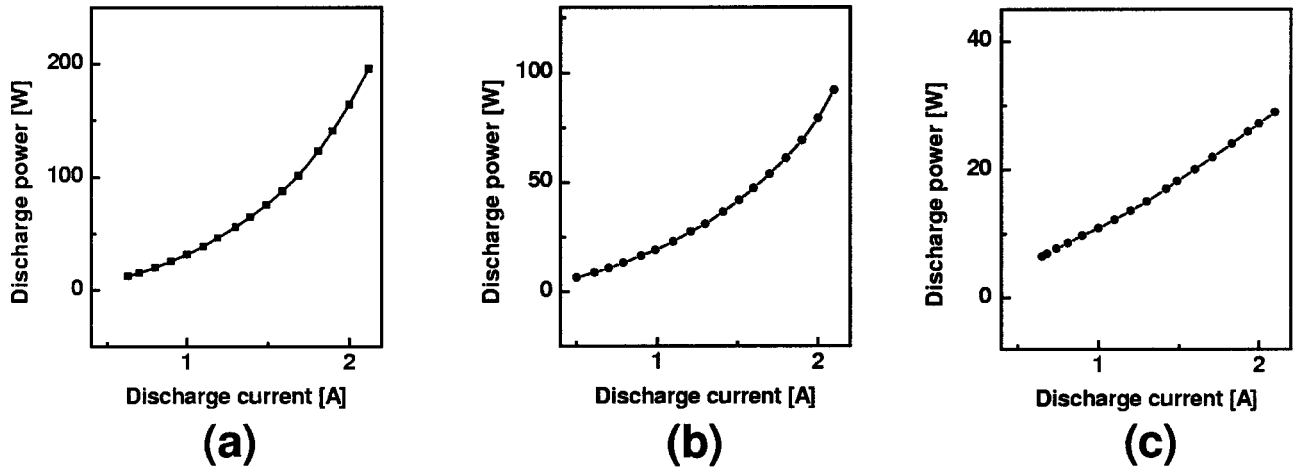

FIG. 2. Discharge power characteristics of (a) 8 MHz, (b) 13.56 MHz, and (c) 29 MHz at 2.67 Pa obtained from the experiments.

by 40 mm and positioned at the center of the discharge chamber. To keep the discharge between the two electrodes, a confinement ring having a diameter equal to that of the electrode and a height of 10 mm is introduced beneath the powered electrode, and each electrode is wrapped by a ceramic cylinder 200 mm in diameter and 50 mm in height. rf power (ENI, *A*1000) is delivered to the powered electrode through a standard L-type matching network and a coaxial cable. The background pressure in the vacuum chamber is in the 10^{-7} Torr range and argon gas flows through the discharge chamber to maintain gas purity during the operation. Electrical characteristic measurements are performed with a current–voltage monitor (ENI.INC, V-I probe) mounted on the powered electrode. The experiments are performed at low pressure (2.67 Pa).

III. EXPERIMENTAL RESULTS AND DISCUSSION

Increasing the driving frequency, we measure the discharge current, voltage, and the phase shift between them at 2.67 Pa. From these experimental data, we obtain the discharge powers and resistances at different driving frequencies, as shown in Figs. 2 and 3. Figure 2 shows the power characteristic of the discharge as a function of the discharge current with different driving frequencies: 8 MHz [Fig. 2(a)], 13.56 MHz [Fig. 2(b)], and 29 MHz [Fig. 2(c)]. The power characteristic of 8 MHz is almost a square function of the discharge current, as shown in Fig. 2(a). As mentioned before, this means that the rf discharge power is mainly consumed by ions in the sheath.[9,11] While increasing the driving frequency, however, the square dependence of power characteristic becomes weaker [Fig. 2(b)] and finally disappears at 29 MHz, so that it seems to be linear, as shown in Fig. 2(c). This change reflects the fact that, the power dissipation mode transition occurs from the ion-dominated dissipation mode to the electron-dominated dissipation mode during the frequency increase.[9,11,10] We can easily see the transition in the resistance characteristics in Fig. 3. An increasing curve of a resistance of 8 MHz [Fig. 3(a)] changes to a monotonously decreasing one as the driving frequency increases [Fig. 3(c)]. This also reflects the transition of the power dissipation mode.[9,11,10] Hence, at 29 MHz, the rf discharge power is mainly consumed by electrons, while at 8 MHz, the rf discharge power is mainly consumed by ions. Therefore, we can conclude that the transition of power dissipation mode from

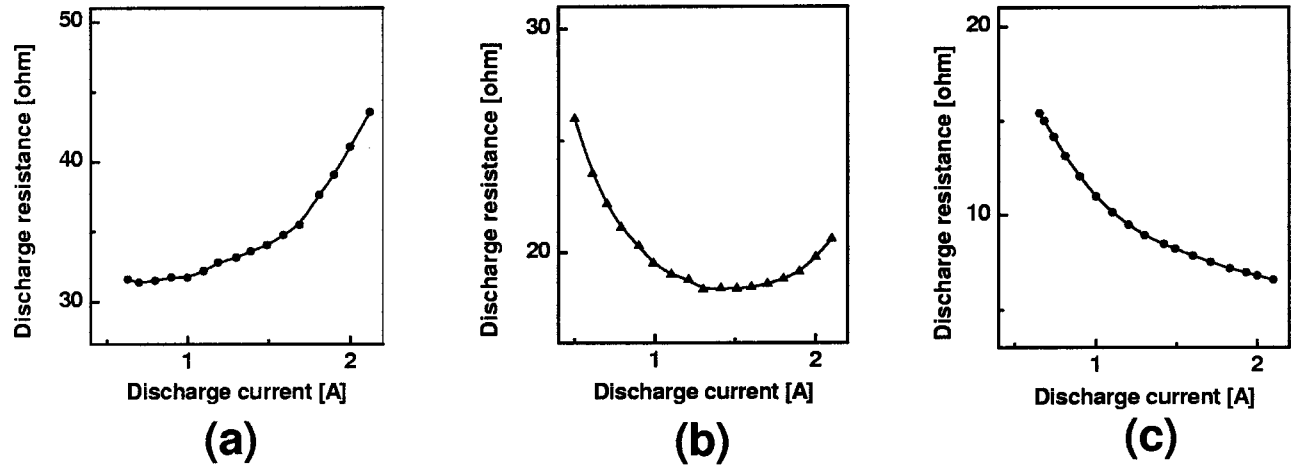

FIG. 3. Discharge resistance characteristics of (a) 8 MHz, (b) 13.56 MHz, and (c) 29 MHz at 2.67 Pa obtained from the experiments.

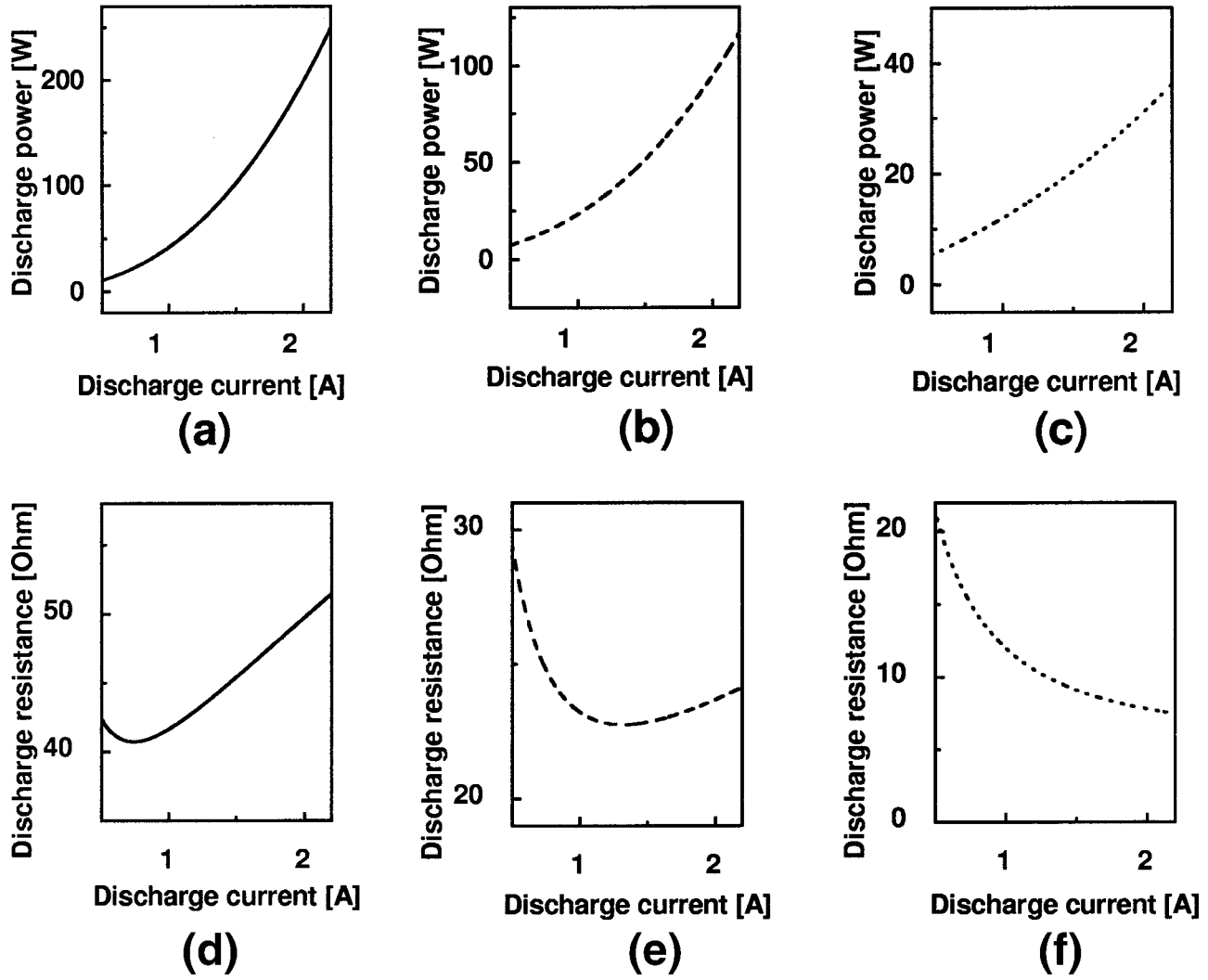

FIG. 4. Discharge power characteristics of (a) 8 MHz, (b) 13.56 MHz, (c) 29 MHz, and discharge resistance characteristics of (d) 8 MHz, (e) 13.56 MHz, (f) 29 MHz at 2.67 Pa [calculated from Eq. (2)].

the ion-dominated dissipation mode to the electron-dominated dissipation mode takes place during the driving frequency increase.

To theoretically investigate the power dissipation mode transition, we use a resistive homogeneous model which was suggested by Schneider[12] and later modified by Godyak[9] to take into account of ion power loss and electron stochastic heating in the sheath. As has previously been shown,[9,11,10,13] the total discharge power can be expressed as

$$P_{\mathrm{tot}} = V_p \cdot I + R_{\mathrm{sh}} \cdot I^2, \tag{1}$$

where I is a rf discharge current in root-mean square (rms) R_{sh}, the sheath resistance, is a function of the discharge current, pressure, and driving frequency, and V_p, an ohmic part

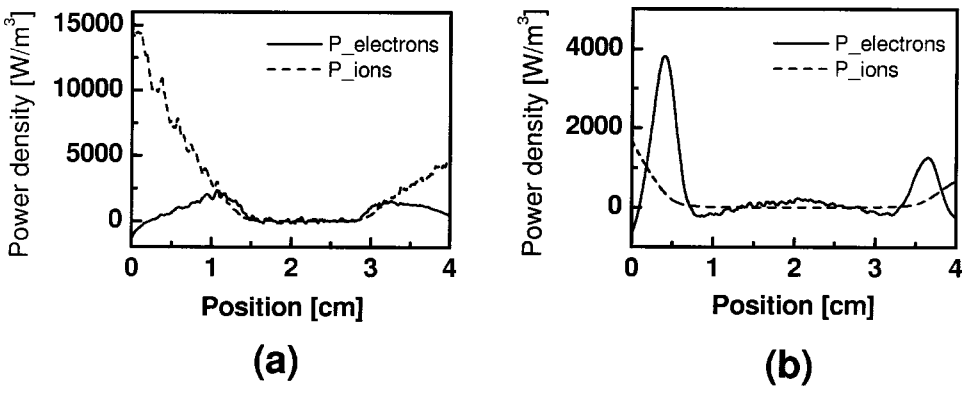

FIG. 5. Spatial profile of the dissipated rf power density of the discharge at 0.3 A with different frequencies (a) 8 MHz and (b) 40 MHz at 2.67 Pa calculated from the PIC simulations.

of the rf voltage across the bulk plasma in rms that includes collisional and stochastic electron heating, is almost independent of current and the driving frequency as a consequence of ionization and energy balance in a weakly ionized gas discharge plasma.[8,11] Each first and second term in Eq. (1) means the dissipated rf power by electrons and ions, respectively, in the capacitive discharge. By using a collisional sheath resistance (Ref. 8), we can get a total discharge power as follows:

$$P_{\mathrm{tot}} = V_p \cdot I + (\sqrt{2})^{5/2} \left(\frac{5}{3\epsilon_0 A} \right)^{3/2} \cdot \left(\frac{2k}{3\sqrt{P_g}} \right) \left(\frac{I}{\omega} \right)^{5/2}, \qquad (2)$$

where A is an area of the discharge electrode, ϵ_0 is a permittivity in vacuum, $k(=103.75\,\mathrm{m}^{3/2}\,\mathrm{Pa}^{1/2}/\mathrm{V}^{1/2}\mathrm{s})$ is a mobility constant,[14,15] P_g is a gas pressure, and ω is a driving frequency. Because, even at 2.67 Pa, the Ar^+ ion mean-free path is shorter than the sheath length, this collisional sheath resistance model is still available in our experiment.[11]

Figure 4 shows the calculated result of Eq. (2) for $A = 1.5\times10^{-2}\,\mathrm{m}^2$, $V_p \approx 10\,\mathrm{V}$ for different frequencies. As shown in Figs. 2–4, the calculated results are qualitatively consistent with the experimental results. In the conventionally used frequency 13.56 MHz, when the discharge current is small, the first term in Eq. (2) is larger than the second one, so that the discharge power characteristic is almost a linear function of the discharge current ($P_{\mathrm{dis}} \sim P_{\mathrm{electrons}} = V_p \cdot I$). But when the discharge current is large, the second term in Eq. (2) is larger than the first one, so that the discharge power characteristic is almost a square function of the discharge current ($P_{\mathrm{dis}} \sim P_{\mathrm{ions}} = R_{\mathrm{sh}} \cdot I^2$).[9] However in low frequency, 8 MHz, although the discharge current is small, the ion-dissipated power is still larger than the electron-dissipated power due to $P_{\mathrm{ions}} \propto 1/\omega^{5/2}$. Thus the power characteristic seems to be a square function of the discharge current. On the contrary, in high frequency 29 MHz, although the discharge current is large, the electron-dissipated power is still larger than the ion-dissipated power, thus the power characteristic seems to be a linear function of the discharge current. As a result, increasing the driving frequency with a fixed discharge current, the power characteristic $[P(I)]$ changes from a square to a linear dependence, and the resistance $[R(I)]$ changes from an increasing curve to a decreasing curve as shown in Figs. 2–4. This means that the power dissipation mode transition takes place from the ion-dominated dissipation to the electron-dominated dissipation during the frequency increase.

To confirm the power dissipation mode transition, we investigate the particle simulation using a modified PIC/Monte Carlo one-dimensional simulation code, XPDC1[16] with time step: 5*e*-12, number of cells: 500, area ratio of two electrodes: 2 (inner radius: 4 cm, outer radius: 8 cm, height: 0.061 26 cm), pressure: 2.67 Pa, secondary electron emission coefficient: 0.2, and current 0.3 A. After steady state, the power densities averaged over a few period are obtained for each species. Figure 5 shows the spatial profile of dissipated rf power density for each species (electrons and ions) at different driving frequencies, 8 MHz [Fig. 5(a)], and 40 MHz [Fig. 5(b)]. While the ion-dissipated power is larger than the electron-dissipated power at 8 MHz [Fig. 5(a)], the electron-dissipated power is larger than the ion-dissipated power at 40 MHz [Fig. 5(b)]. Therefore, as we have expected in the experiment, the power dissipation mode transition occurs during the driving frequency increase as shown in Fig. 6.

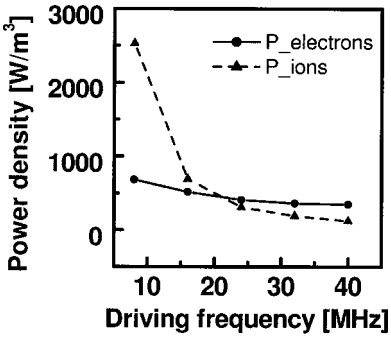

FIG. 6. Spatially averaged dissipated rf power density of the discharge at 0.3 A, at 2.67 Pa against the different frequencies calculated from the PIC simulation.

IV. CONCLUSION

In conclusion, through electrical measurements of the capacitive discharge at various driving frequencies, we observed the transition of the power dissipation mode induced by the driving frequency increase. Because the sheath resistance and ion-dissipated power in the sheath decrease with the driving frequency, the power dissipation mode transition takes place from the ion-dominated power dissipation to the electron-dominated power dissipation during the frequency increase. We experimentally verify the power dissipation mode transition induced by a driving frequency, which is briefly suggested by Beneking and Godyak in their studies,[8,11] by means of electrical measurement of the discharge. Furthermore, through using the simple power dissipation model including the collisional sheath model and the PIC simulation, we can theoretically evaluate the transition.

ACKNOWLEDGMENTS

This work was sponsored in part by the SYSTEM I.C. 2010 of the Ministry of Science and Technology (MOST) and the Ministry of Commerce, Industry, and Energy (MOCIE) and by a grant from the Interdisciplinary Research Program of KOSEF. This work was also supported in part by the National Research Laboratory Project of Korea (M1-0104-00-0071). One of the authors would like to thank Plasmart Inc. for its technical and financial support for this work.

[1] Y. Catherin, C. R. Acad. Sci. **273**, 588 (1971).
[2] B. Chapman, *Glow Discharge Process* (Wiley, New York, 1980), Chap. 5.
[3] K. Takaki, D. Taguchi, and T. Fujiwara, Appl. Phys. Lett. **78**, 2646 (2001).
[4] S. V. Berezhnoi, I. K. Kaganovich, and L. D. Tsendin, Plasma Phys. Rep. **24**, 556 (1998).
[5] M. M. Turner, D. A. W. Hutchinson, R. A. Doyle, and M. B. Hopkins, Phys. Rev. Lett. **76**, 2069 (1996).
[6] V. A. Godyak, R. B. Piejak, and B. M. Alexandrovich, Plasma Sources Sci. Technol. **1**, 36 (1992).
[7] V. A. Godyak, R. B. Piejak, and B. M. Alexandrovich, Phys. Rev. Lett. **68**, 40 (1992).

[8] C. Beneking, J. Appl. Phys. **68**, 4461 (1990).
[9] V. A. Godyak, R. B. Piejak, and B. M. Alexandrovich, IEEE Trans. Plasma Sci. **19**, 660 (1991).
[10] S. J. You, C. W. Chung, K. H. Bai, and H. Y. Chang, Appl. Phys. Lett. **81**, 2529 (2002).
[11] V. A. Godyak, P. B. Piejak, and B. M. Alexandrovich, J. Appl. Phys. **69**, 3455 (1991).
[12] F. Schneider, Z. Angew. Phys. **6**, 839 (1949).
[13] V. A. Godyak and N. Sternberg, Phys. Rev. A **42**, 2299 (1990).
[14] L. S. Frost, Phys. Rev. **105**, 354 (1957).
[15] S. C. Brown, *Basic Data of Plasma Physics* (Wiley, New York, 1994), p. 65.
[16] J. P. Verboncoeur, M. V. Alves, V. Vahedi, and C. K. Birdsall, J. Comput. Phys. **104**, 321 (1993).